

# Resonating Valence Bond Theory of Superconductivity for Dopant Carriers: Application to the Cobaltates

Alvaro Ferraz

*International Center of Condensed Matter Physics, Universidade de Brasilia,  
Caixa Postal 04667, 70910-900 Brasilia, DF, Brazil*

Evgueny Kochetov

*Bogolyubov Theoretical Laboratory, Joint Institute for Nuclear Research, 141980 Dubna, Russia*

Marcin Mierzejewski

*Department of Theoretical Physics, Institute of Physics, University of Silesia, 40-007 Katowice, Poland*

Within the t-J model hamiltonian we present a new RVB mean field theory directly in terms of dopant particles. We apply this theory to  $\text{Na}_x\text{CoO}_2 \cdot y\text{H}_2\text{O}$  and show that it reproduces several important features of the observed data for this compound.

## I. INTRODUCTION

The remarkable discovery of superconductivity in  $\text{Na}_x\text{CoO}_2 \cdot y\text{H}_2\text{O}$  for  $x = 0.35$  and  $y = 1.30$  by Takada *et al.*<sup>1</sup> attracted a lot of attention. The experimental findings indicate several striking similarities between the cobaltates and the cuprates.  $\text{Na}_x\text{CoO}_2 \cdot y\text{H}_2\text{O}$  can be viewed as a 2d Mott insulator. The  $\text{Co}$  atoms form a triangular lattice but  $\text{Co}^{4+}$  is in a  $s = \frac{1}{2}$  low spin state. The transition temperature ( $T_c$ ) is seen to decrease for both underdoped and overdoped materials<sup>2</sup> although for the cobaltates the maximum  $T_c$  is much lower ( $T_c \approx 5\text{K}$ ) and the optimal doping is twice as large as in the cuprates. Finally, as one varies temperature and electron concentration, apart from superconductivity, there are observed unusual electronic properties<sup>3</sup> and clear hints that strong electronic correlation is at work in both cases.

All this turns attractive the application of the resonating valence bond (RVB) ideas to this new compound. Baskaran<sup>4</sup> was the first to present qualitative arguments in favor of the RVB approach for the cobaltates. Soon after that Kumar and Shastry<sup>5</sup> as well as Lee and coworkers<sup>6,7</sup> presented their first estimates for the mean field (MF) phase diagram,  $T_c$  versus doping, in a RVB framework. In the cobaltates the  $\text{CoO}_2$  layers are arranged in a triangular lattice which naturally exhibits considerable magnetic frustration. This not only brings modifications to the symmetry of the resulting superconducting state, as pointed out by others<sup>4,5,6,7,8</sup>, but makes the the application of a MF RVB, to reproduce the experimental findings related to the superconductivity of  $\text{Na}_x\text{CoO}_2 \cdot y\text{H}_2\text{O}$ , even more challenging. The reasons for that are as follows. The maximum  $T_c$  for the  $\text{CoO}_2$  layers occurs for doping values nearly twice as large as in the cuprates. This might be indicative that the phase fluctuations of the superconducting (SC) order parameter could be much too strong for the stability of the MF RVB state. Moreover, in the standard approach low doping is always favored and makes even harder a more

quantitative agreement with experiment in the case of the cobaltates.

Within the original Baskaran-Zou-Anderson (BZA) MF approximation<sup>9</sup> a non-zero value of the RVB MF order parameter (OP) does not by itself imply superconductivity. The true SC OP in their approach is essentially taken as a product of a spinon (a spin-1/2 neutral fermion) pairing OP and a bose condensation factor for the holons (spin-0 charged bosons)<sup>10</sup>, following the more conventional slave-boson approximation. The phase of the OP accounts for the fluctuations which drives  $T_c$  to zero at zero doping. The bose condensation temperature for the holons is estimated separately and the region in which both the spin-pairing OP and the mentioned holon bose factor are non-zero determines the resulting RVB superconducting phase<sup>5</sup>. All this seems to indicate that the standard MF RVB basic ingredients – the lattice spin singlet pairs – which might indeed be appropriate to describe the physics at very low dopings is not the best starting point to address the superconducting regime at higher doping values.

To overcome those limitations we present a new RVB MF scheme which takes direct account of the dopant particles themselves and treats the non-double occupancy (NDO) constraint beyond the conventional slave-boson mean field approximation. As will be demonstrated by this and later works this new RVB representation is most suitable to deal with cases in which strongly correlated electronic superconductivity is manifest in both low and high doping regimes.

In this first work we apply our new method to the  $\text{CoO}_2$  superconductors. Our starting point is the t-J model on a triangular lattice. In doing that we follow the arguments which consider the 3d levels of the  $\text{Co}^{4+}$  ions being crystal field split in the  $\text{CoO}_2$  layers producing singly occupied non-degenerate spin-1/2  $d_{z^2}$  orbitals. Those orbitals are directly associated with the singlet states in our t-J model representation based on the Hubbard X operators. The use of that representation will

allow us to go beyond the conventional treatment of the NDO constraint. The  $X$  operators are later given in a convenient coherent-state path integral representation. The resulting variables in this representation are naturally split into bosonic and fermionic degrees of freedom. The bosonic modes correspond to  $SU(2)$  spin excitations while the fermion variables are spinless and describe  $U(1)$  charge excitations instead. Combining those spinon amplitudes and spinless fermion parameters together we then construct appropriate fermionic fields which carry both spin and charge degrees of freedom and can be directly related to the dopant carriers in the t-J model. We are able in this way to take a direct account of the doping dependence of the critical superconducting temperature preserving all the symmetry properties of the t-J hamiltonian.

We reformulate the RVB theory of the SC phase entirely in terms of those quasiparticle states and use this new scheme initially to describe the superconducting properties of the cobaltates. We find qualitatively good agreement with experiment and we are able for the first time to reproduce the observed dome structure of the  $T_c$  versus doping phase diagram for those materials in a RVB MF framework. The application of our RVB method to the cuprates will be presented in a subsequent work.

## II. T-J HAMILTONIAN AND THE NDO CONSTRAINT

We start by expressing the  $t$ - $J$  Hamiltonian<sup>11</sup>

$$H_{t-J} = -t \sum_{ij\sigma} c_{i\sigma}^\dagger c_{j\sigma} + h.c. + J \sum_{ij} \left( \vec{Q}_i \vec{Q}_j - \frac{1}{4} n_i n_j \right), \quad (1)$$

with the NDO constraint,  $\sum_\sigma n_{i\sigma} \leq 1$ , in terms of the Hubbard operators<sup>12</sup>,

$$X_i^{\sigma 0} = c_{i\sigma}^+ (1 - n_{i,-\sigma}), \quad n_{i,-\sigma} n_{i,\sigma} = 0.$$

Here  $c_{i\sigma}$  is the electron annihilation operator at site  $i$  with the spin projection  $\sigma = \uparrow, \downarrow$ ,  $n_{i\sigma} = c_{i\sigma}^\dagger c_{i\sigma}$ , and the  $\vec{Q}$ 's are the corresponding electron spin operators. In terms of these operators the local NDO constraint holds rigorously and the  $t$ - $J$  model becomes

$$H_{t-J} = -t \sum_{ij\sigma} X_i^{\sigma 0} X_j^{0\sigma} + h.c. + J \sum_{ij} \left( \vec{Q}_i \vec{Q}_j - \frac{1}{4} n_i n_j \right), \quad (2)$$

where the electron spin operator now reads  $\vec{Q}_i = \frac{1}{2} \sum_{\sigma\sigma'} X_i^{\sigma 0} \vec{\tau}_{\sigma\sigma'} X_i^{0\sigma'}$ , with the  $\vec{\tau}$ 's being Pauli matrices.

Fermionic operators  $X_i^{\sigma 0}$  project the electron creation operators onto a space spanned by the basis  $\{|0\rangle_i, |\sigma\rangle_i\}$  and take the form  $X_i^{\sigma 0} = |\sigma\rangle_i \langle 0|_i$ . Together with the bosonic generators,  $X_i^{\sigma\sigma'} = |\sigma\rangle_i \langle \sigma'|_i$  the full set of operators  $X_i^{ab}$ ,  $a, b = 0, \uparrow, \downarrow$  forms, on every lattice site, a

basis of the fundamental representation of the semisimple doubly graded Lie algebra  $su(2|1)$  given by the (anti)commutation relations

$$\{X_i^{ab}, X_j^{cd}\}_\pm = (X_i^{ad} \delta^{bc} \pm X_j^{bc} \delta^{ad}) \delta^{ij},$$

where the (+) sign should be used only when both operators are fermionic.

Since  $su(2|1)$  can be viewed as a supergeneralization of the conventional spin  $su(2)$  algebra, the t-J Hamiltonian appears as a superextension of the Heisenberg magnetic hamiltonian, with a hole being a superpartner of a  $su(2)$  magnetic excitation<sup>13</sup>. This superalgebra can also be thought of as a natural generalization of the standard fermionic algebra spanned by generators  $c_\sigma^+, c_\sigma$ , and unity  $I$ , to the case where the fermionic operators are subject to the NDO constraint. The incorporation of this constraint manifests itself in more complicated commutation relations between  $X$  operators in comparison with those produced by the conventional fermionic operators. Note that the Gutzwiller projection  $P_G = \prod_i (1 - n_{\sigma i} n_{-\sigma i})$  that excludes the doubly occupied state  $|\uparrow\downarrow\rangle$  is equivalent to the Hubbard operator representation, since  $P_G c_{\sigma i}^+ c_{\sigma j} P_G = X_i^{\sigma 0} X_j^{0\sigma}$ .

Note also that the occupation constraint is different for the hole and electron doping. To treat them in a unique way we perform, for electron dopings, a canonical particle-hole transformation  $c_{i\sigma} \rightarrow c_{i-\sigma}^+$  that restores the non-double occupancy constraint but reverses the sign of  $t$ . Using then the Hubbard operator representation in terms of the transformed  $c$ -operators we again arrive at Eq.(2) with, however,  $t \rightarrow -t$ . Although the  $CoO_2$  layer is an electron doped Mott insulator we shall for convenience formally deal with the more familiar case of hole doping making the necessary changes only at the end of our work.

Since the  $X$  operators are generators of the  $su(2|1)$  superalgebra we are lead naturally to employ the  $su(2|1)$  coherent-state path-integral representation of the t-J partition function. There are a few rationales to do that. First, this provides a mathematical setting well adjusted to address the t-J model with the crucial constraint of no double occupancy naturally built in the formalism from the very beginning. Second, within the  $su(2|1)$  path-integral representation the associated effective t-J action lives on a natural classical phase space of the t-J model – the  $SU(2|1)$  homogeneous compact manifold,  $CP^{1|1}$  (see below). The group  $SU(2|1)$  acts on the  $CP^{1|1}$  manifold as a group of canonical transformations in a way that the transformation properties of the basic fields - the local coordinates on  $CP^{1|1}$  - can be easily found. Third, these coordinates are naturally split into bosonic and fermionic degrees of freedom. In the context of the t-J model the bosonic fields correspond to the  $SU(2)$  spin excitations whereas the fermionic ones are spinless and may be used to describe the  $U(1)$  charge excitations. This provides a natural setting to implement the spin-charge separation inherent in the spin liquid phase at least in 1D. Finally, the transformation properties of the  $CP^{1|1}$  coordinates

under global  $SU(2) \times U(1)$  rotations - the exact symmetry of the t-J hamiltonian - imply that their certain combinations transform in the linear spinor representations of  $SU(2)$  and may therefore be used to describe fermionic quasiparticle excitations that carry both the charge and spin quantum numbers. We show that such quasiparticles arise as the dopant particles in the t-J model relevant for describing the SC phase. In particular, we formulate the RVB theory of the SC phase of the t-J model directly in terms of the dopant particles and apply it to describe the SC in the cobaltates.

### III. $SU(2|1)$ COHERENT STATES AND PATH INTEGRAL

The normalized  $su(2|1)$  coherent state (CS) associated with the 3D fundamental representation takes the form

$$|z, \xi\rangle = (1 + \bar{z}z + \bar{\xi}\xi)^{-1/2} \exp(zX^{1\dagger} + \xi X^{0\dagger}) |\uparrow\rangle, \quad (3)$$

where  $z$  is a complex number, and  $\xi$  is a complex Grassmann parameter. The set  $(z, \xi)$  can be thought of as local coordinates of a given point on  $CP^{1|1}$ . This supermanifold appears as a  $N = 1$  superextension of a complex projective plane, or ordinary two-sphere,  $CP^1 = S^2$ , to accommodate one extra complex Grassmann parameter<sup>14</sup>. At  $\xi = 0$ , the  $su(2|1)$  CS reduces to the ordinary  $su(2)$  CS,  $|z, \xi = 0\rangle \equiv |z\rangle$  parametrized by a complex coordinate  $z \in CP^1$ . Note that the classical phase space of the Hubbard operators,  $CP^{1|1}$ , appears as a  $N = 1$  superextension of the CS for the  $su(2)$  spins.

In the basis  $|z, \xi\rangle = \prod_j |z_j, \xi_j\rangle$ , the  $t-J$  partition function takes the form of the  $su(2|1)$  CS phase-space path integral,

$$Z_{t-J} = \text{tr} \exp(-\beta H_{t-J}) = \int_{CP^{1|1}} D\mu_{SU(2|1)}(z, \xi) e^{S_{t-J}}, \quad (4)$$

where

$$D\mu_{SU(2|1)}(z, \xi) = \prod_{j,t} \frac{d\bar{z}_j(t)dz_j(t)}{2\pi i} \frac{d\bar{\xi}_j(t)d\xi_j(t)}{1 + |z_j|^2 + \bar{\xi}_j\xi_j}$$

stands for the  $SU(2|1)$  invariant measure with the boundary conditions,  $z_j(0) = z_j(\beta)$ ,  $\xi_j(0) = -\xi_j(\beta)$ . The t-J effective action on  $CP^{1|1}$  now reads  $S_{t-J} = -\int_0^\beta \langle z, \xi | d/dt + H_{t-J} | z, \xi \rangle dt$ , which gives

$$S_{t-J} = \frac{1}{2} \sum_j \int_0^\beta \frac{\dot{\bar{z}}_j z_j - \bar{z}_j \dot{z}_j + \dot{\bar{\xi}}_j \xi_j - \bar{\xi}_j \dot{\xi}_j}{1 + |z_j|^2 + \bar{\xi}_j\xi_j} dt - \int_0^\beta H_{t-J}^{cl} dt. \quad (5)$$

The first part of the action (5) is a purely kinematical term that reflects the geometry of the underlying phase

space while the classical image of the hamiltonian (2) becomes an average value of  $H_{t-J}$  over the  $su(2|1)$  coherent states,

$$\begin{aligned} H_{t-J}^{cl} &= \langle z, \xi | H_{t-J} | z, \xi \rangle \\ &= -t \sum_{ij} \frac{\xi_i \bar{\xi}_j (1 + z_j \bar{z}_i) + h.c.}{(1 + |z_i|^2 + \bar{\xi}_i \xi_i)(1 + |z_j|^2 + \bar{\xi}_j \xi_j)} \\ &\quad + J \sum_{ij} \frac{-|z_i|^2 - |z_j|^2 + z_i z_j + \bar{z}_i \bar{z}_j}{(1 + |z_i|^2 + \bar{\xi}_i \xi_i)(1 + |z_j|^2 + \bar{\xi}_j \xi_j)}. \end{aligned} \quad (6)$$

The fact that the electron system with the NDO constraint lives on the compact manifold, supersphere  $CP^{1|1}$  can be explained as follows. Let us for a moment suppose that the so-called slave-fermion representation for the electron operators is used, i.e.,  $c_\sigma = f a_\sigma^+$ , where  $f$  is a spinless fermionic operator, whereas  $a_\sigma$  is the spinful boson. The NDO constraint now reads  $\sum_\sigma a_\sigma^+ a_\sigma + f^+ f = 1$ . Within the slave-fermion path integral representation

$$Z_{t-J} = \int D\mu_{flat} e^{S_{t-J}(\bar{a}_\sigma, a_\sigma, f)}, \quad (7)$$

with the integration measure  $D\mu_{flat} = \prod_i D\bar{a}_{i\uparrow} D a_{i\uparrow} D\bar{a}_{i\downarrow} D a_{i\downarrow} D\bar{f}_i D f_i$ , this constraint transforms into

$$\sum_\sigma \bar{a}_{i\sigma} a_{i\sigma} + \bar{f}_i f_i = 1, \quad (8)$$

with  $a_\sigma$  and  $f$  standing now for complex numbers and complex Grassmann parameters, respectively. Equation (8) is exactly that for the supersphere  $CP^{1|1}$  embedded into a flat superspace. Any mean-field treatment of (7) should respect this constraint, which, however, poses a severe technical problem. If one however resolves this equation explicitly by making the identifications

$$\begin{aligned} a_\uparrow &= \frac{1}{\sqrt{1 + \bar{z}z + \bar{\xi}\xi}}, \quad a_\downarrow = \frac{z}{\sqrt{1 + \bar{z}z + \bar{\xi}\xi}}, \\ f &= \frac{\xi}{\sqrt{1 + \bar{z}z + \bar{\xi}\xi}}, \end{aligned} \quad (9)$$

one can further treat the variables  $z, \xi$  as if they were indeed free of any constraints. Substitution of (9) into (7) results in the  $su(2|1)$  path-integral representation of  $Z_{t-J}$  given by (4). Geometrically, the set  $(z, \xi)$  appears as local (projected) coordinates of a point on the supersphere defined by equation (8).

Representation (4)-(6) rigorously incorporates the local NDO constraint at the apparent expense of a more complicated compact phase space for the projected electron operators.

### IV. SYMMETRY

At the supersymmetric point,  $J = 2t$ , the  $t-J$  model Hamiltonian is known to exhibit a global  $SU(2|1)$  symmetry. Away from that point this symmetry reduces to

$SU(2) \times U(1) \subset SU(2|1)$ . This symmetry group acts on a point  $(z(t), \xi(t)) \in CP^{1|1}$  in a way that,

$$\begin{aligned} z(t) \rightarrow z_g(t) &= \frac{uz(t) + v}{-\bar{v}z(t) + \bar{u}}, \quad g \in SU(2) \times U(1), \\ \xi(t) \rightarrow \xi_g(t) &= \frac{e^{i\theta}\xi(t)}{-\bar{v}z(t) + \bar{u}}, \end{aligned} \quad (10)$$

where the group parameters are to be taken to be site independent:

$$\begin{pmatrix} u & v \\ -\bar{v} & \bar{u} \end{pmatrix} \in SU(2), \quad e^{i\theta} \in U(1). \quad (11)$$

It can easily be checked that both the  $SU(2|1)$  measure and the effective action (5) are invariant under the group transformations (10), so that the representation of the partition function (4) remains intact. Notice that (10) appears as a covariant reparametrization of  $CP^{1|1}$ . However, one can in principle employ any other reparametrization, not necessarily of the form of the  $SU(2|1)$  action on  $CP^{1|1}$ . We are interested in the one that decouples the  $SU(2|1)$  measure factor into the  $SU(2)$  spin and the  $U(1)$  spinless fermion measures,

$$\begin{aligned} D\mu_{SU(2)}(\bar{z}, z) &= \prod_{j,t} \frac{d\bar{z}_j(t)dz_j(t)}{2\pi i(1+|z_j(t)|^2)^2}, \\ D\mu_{U(1)}(\bar{\xi}, \xi) &= \prod_{j,t} d\bar{\xi}_j(t)d\xi_j(t), \end{aligned} \quad (12)$$

respectively.

Such a reparametrization can be taken to be

$$z \rightarrow z, \quad \xi \rightarrow \xi\sqrt{1+|z|^2}. \quad (13)$$

Up to an inessential factor which redefines a chemical potential, we get

$$D\mu_{su(2|1)} \rightarrow D\mu_{su(2)}(\bar{z}, z) \times D\mu_u(1)(\bar{\xi}, \xi), \quad (14)$$

and the effective action becomes

$$\begin{aligned} S_{t-J} \rightarrow S_{t-J} &= \frac{1}{2} \sum_i \int_0^\beta \frac{\bar{z}_i z_i - \bar{z}_i \dot{z}_i}{1 + \bar{z}_i z_i} (1 - \bar{\xi}_i \xi_i) dt \\ &+ \frac{1}{2} \sum_i \int_0^\beta (\bar{\xi}_i \xi_i - \bar{\xi}_i \dot{\xi}_i) dt - \int_0^\beta \tilde{H}_{t-J}^{cl}(t) dt, \end{aligned} \quad (15)$$

with

$$\begin{aligned} \tilde{H}_{t-J}^{cl} &= -t \sum_{ij} (\xi_i \bar{\xi}_j \langle z_i | z_j \rangle + h.c.) \\ &+ \frac{J}{2} \sum_{ij} (|\langle z_i | z_j \rangle|^2 - 1) (1 - \bar{\xi}_i \xi_i) (1 - \bar{\xi}_j \xi_j). \end{aligned} \quad (16)$$

Here  $\langle z_i | z_j \rangle$  stands for an inner product of the  $su(2)$  coherent states,

$$\langle z_i | z_j \rangle = \frac{1 + \bar{z}_i z_j}{\sqrt{(1 + |z_j|^2)(1 + |z_i|^2)}}.$$

From eqs. (10) one can infer the transformation properties of the new  $CP^{1|1}$  coordinates (13) under a global  $SU(2) \times U(1)$  action:

$$\begin{aligned} z(t) \rightarrow z_g(t) &= \frac{uz(t) + v}{-\bar{v}z(t) + \bar{u}}, \quad g \in SU(2) \times U(1), \\ \xi(t) \rightarrow \xi_g(t) &= e^{i\Phi_g + i\theta}\xi(t), \end{aligned} \quad (17)$$

where

$$i\Phi_g = \log \sqrt{\frac{-v\bar{z} + u}{\bar{v}z + \bar{u}}}.$$

Note also that  $|z\rangle \rightarrow |z\rangle_g = e^{-i\Phi_g}|z_g\rangle$ . It can be straightforwardly checked that both the measure and the t-J action (15) remain invariant under the action of  $SU(2) \times U(1)$  (17).

The following remarks are needed at this stage. First, in spite of the fact that the function  $i\Phi_g$  bears a site-dependence through the  $z_i$  fields, the transformation (17) is a global one: the group parameters  $(u, v)$  are site-independent. Second, although the measure factor gets decomposed into the  $su(2)$  spin and spinless fermion pieces, the underlying phase space is not reduced into a direct product of the classical spin and a flat fermionic phase spaces. The function  $\Phi_g$  that enters the transformation law for the fermions also depends on the spinon coordinates,  $z_i(t)$ . Besides, the symplectic one-form (kinetic term) in the effective action (15) is not a simple sum of purely fermionic and spin contributions. This means physically that, in general, the corresponding field excitations are not independent of each other.

## V. EFFECTIVE ACTION

The spinon amplitudes  $z_i(t)$  and the spinless fermion parameters,  $\xi_i(t)$ , are in fact related to each other by the  $SU(2)$  transformation laws (17). From this it follows that we can construct classical images<sup>16</sup> for the operators that describe doped holes. In this respect we make the following ansatz:

$$\begin{aligned} \Psi_\downarrow &= \frac{\xi}{\sqrt{1+|z|^2}}, \quad \bar{\Psi}_\downarrow = \frac{\bar{\xi}}{\sqrt{1+|z|^2}}, \\ \Psi_\uparrow &= \frac{\bar{z}\xi}{\sqrt{1+|z|^2}}, \quad \bar{\Psi}_\uparrow = \frac{z\bar{\xi}}{\sqrt{1+|z|^2}}. \end{aligned} \quad (18)$$

It then follows that  $\bar{\Psi}_\uparrow \Psi_\uparrow + \bar{\Psi}_\downarrow \Psi_\downarrow = \bar{\xi}\xi = \hat{\delta}^{cl}$ , where  $\hat{\delta}^{cl}$  stands for a classical image of the hole-number operator  $\hat{\delta} = 1 - \hat{n}_e = 1 - \sum_\sigma X^{\sigma\sigma}$ . Therefore the resulting fermionic amplitudes describe the propagation of doped holes restricted to the NDO constraint. In view of the group transformations  $SU(2) \times U(1)$  for  $z(t)$  and  $\xi(t)$  the  $\Psi_\sigma$  amplitudes transform in a *linear* spinor representation of  $SU(2)$ ,  $g \rightarrow U_{\bar{g}}$ , as true fermionic amplitudes. Namely,

$$\begin{pmatrix} \Psi_\uparrow \\ \Psi_\downarrow \end{pmatrix} \rightarrow \begin{pmatrix} \bar{u} & \bar{v} \\ -v & u \end{pmatrix} \begin{pmatrix} \Psi_\uparrow \\ \Psi_\downarrow \end{pmatrix} \quad (19)$$

In terms of the  $\Psi_\sigma$  and  $z$  amplitudes we get the corresponding *exact* representation of the  $t$ – $J$  partition function,

$$Z_{t-J} = \int D\mu_{SU(2)}(\bar{z}, z) D\mu_{U(1)}(\bar{\Psi}, \Psi) \exp S \times \prod_i \delta \left( \frac{\Psi_{\uparrow i} - \bar{z}_i \Psi_{\downarrow i}}{\sqrt{1 + |z_i|^2}} \right) \delta \left( \frac{\bar{\Psi}_{\uparrow i} - z_i \bar{\Psi}_{\downarrow i}}{\sqrt{1 + |z_i|^2}} \right), \quad (20)$$

where

$$S = S_{kin} - \int_0^\beta \tilde{H}_{t-J}^{cl}(t) dt. \quad (21)$$

The  $SU(2)$  invariant product of the  $\delta$ -functions ensures the preservation of the correct number of degrees of freedom. The square roots in the  $\delta$ -function arguments come from the evaluation of the Jacobian. In this new dopant carrier representation the kinetic term,

$$S_{kin} = \frac{1}{2} \sum_{\sigma i} \int_0^\beta \left( \bar{\Psi}_\sigma \Psi_\sigma - \bar{\Psi}_\sigma \dot{\Psi}_\sigma \right) dt + \frac{1}{2} \sum_i \int_0^\beta \frac{\bar{z}_i z_i - \bar{z}_i \dot{z}_i}{1 + \bar{z}_i z_i} dt, \quad (22)$$

is nicely decoupled into purely fermionic and spinon parts. It is clear that the fermionic symplectic one-form (the first term in (22)) determines a standard fermionic symplectic structure  $\sum_\sigma d\bar{\Psi}_\sigma \wedge d\Psi_\sigma$  which in turn determines the standard Poisson brackets relations  $\{\bar{\Psi}_\sigma, \Psi_{\sigma'}\}_{PB} = \delta_{\sigma, \sigma'}, \{\Psi_\sigma, \Psi_{\sigma'}\}_{PB} = 0$ . As a result the corresponding operators  $\Psi_\sigma^+, \Psi_{\sigma'}$  describe indeed well-defined fermionic excitations - in our case, doped holes.

As a result, using the new fermion fields, the Hamiltonian that corresponds to  $\tilde{H}_{t-J}^{cl}$  takes the form

$$H_{t-J} = t \sum_{ij\sigma} \Psi_{i\sigma}^+ \Psi_{j\sigma} + h.c. + J \sum_{ij} \left[ (\bar{S}_i \bar{S}_j - \frac{1}{4}) - (\bar{S}_i \bar{M}_j + \bar{S}_j \bar{M}_i) + (\bar{M}_i \bar{M}_j - \frac{1}{4} \hat{\delta}_i \hat{\delta}_j) \right], \quad (23)$$

where we have dropped the tilda sign. The components of the operator of spinon magnetic moment  $\bar{S}$  are the  $su(2)$  generators in the  $s = \frac{1}{2}$  representation. Their classical images are the components of  $\bar{\mathbf{S}}^{cl} = \langle z | \bar{\mathbf{S}} | z \rangle$  with  $S_{cl}^2 = \frac{1}{4}$ . The hole spin operator  $\bar{M} = \frac{1}{2} \sum_\sigma \Psi_\sigma^+ \vec{\tau}_{\sigma\sigma} \Psi_\sigma$ ,  $\bar{M}^2 = \frac{3}{4} \hat{\delta} (2 - \hat{\delta})$ ,  $\hat{\delta} = \Psi_\uparrow^+ \Psi_\uparrow + \Psi_\downarrow^+ \Psi_\downarrow$ , transforms under (17), as a  $SU(2)$  vector while the total Hamiltonian (23) is a  $SU(2)$  scalar. It can also be checked that the electron spin moment is a linear combination of the above two operators:  $\bar{Q} = \bar{S} - \bar{M}$ . For a half-filled band, the Hamiltonian reduces to  $H_{t-J} = J \sum_{ij} (\bar{S}_i \bar{S}_j - \frac{1}{4})$ . If we integrate out the fields  $\Psi_{\uparrow i}, \bar{\Psi}_{\uparrow i}$  in Eq. (20), with the help of the  $\delta$ -functions, we will return to our initial representation as given in Eq. (15).

## VI. SC PHASE

The RVB mean field treatment of the SC phase of the Hamiltonian (23) is now based on the following assumptions:

i) the global  $SU(2) \times U(1)$  symmetry is spontaneously broken by a local order parameter down to  $SU(2)$ . The  $SU(2)$  symmetry is the exact symmetry of the SC phase; ii) the dynamics of the SC phase is governed by the BCS-type dynamics of the valence bond hole  $SU(2)$  singlet pairs and is determined by the linearized quartic hole–hole interaction  $J \sum_{ij} (\bar{M}_i \bar{M}_j - \frac{1}{4} \hat{\delta}_i \hat{\delta}_j)$  as well as by the hopping term. The hole spin singlets interact with the quasiclassical spinon background  $J \sum_{ij} (\bar{S}_i \bar{S}_j - \frac{1}{4})$  via the induced moment–moment interaction  $-J \sum_{ij} \bar{S}_i \bar{M}_j$ . This can be treated within the MF approximation as well; iii) the spinon–spinon and hole–spinon interactions, in first order approximation, take the form  $\bar{S}_i \bar{S}_j \simeq \langle \bar{S}_i \rangle \bar{S}_j + \dots, \bar{S}_i \bar{M}_j \simeq \langle \bar{S}_i \rangle \bar{M}_j + \bar{S}_i \langle \bar{M}_j \rangle + \dots$ . We ignore, at first, quantum fluctuations of the spinon field compared to the ones originated by the  $\Psi$ –field. In contrast, for the cuprates the  $\langle \bar{S}_i \bar{M}_j \rangle$  correlation functions seem to be of crucial importance and should therefore be treated beyond a MF approximation. This is confirmed by the recent observation of antiferromagnetic ordering associated with the superconducting vortex cores<sup>17</sup>; iv) due to the presence of the  $SU(2)$  invariance, the  $S$  dependent term naturally drops out of the MF Hamiltonian; v) the constrained RVB hole–singlet annihilation operator takes the form  $B_{ij} = \Psi_{i\uparrow} \Psi_{j\downarrow} - \Psi_{i\downarrow} \Psi_{j\uparrow}$ ,  $B_{ii} = 0$ . In the SC phase the  $U(1)$  global symmetry  $\Psi_{j\sigma} \rightarrow e^{i\theta} \Psi_{j\sigma}$  is spontaneously broken by the local  $SU(2)$  invariant order parameter  $\Delta_{ij} = \langle B_{ij} \rangle$ .

The  $t$ – $J$  Hamiltonian in this way reduces to

$$H_{t-J}^{SC} = t \sum_{ij\sigma} \Psi_{i\sigma}^+ \Psi_{j\sigma} + h.c. + \frac{JNZ|\Delta|^2}{4} - \hat{N}_e \mu + \frac{J}{2} \sum_{ij} (\Psi_{i\uparrow} \Psi_{j\downarrow} - \Psi_{i\downarrow} \Psi_{j\uparrow}) \bar{\Delta}_{ij} + h.c. \quad (24)$$

where the chemical potential  $\mu$  has been introduced to control the number of electrons,  $\hat{N}_e = N - \sum_{\sigma i} \Psi_{i\sigma}^+ \Psi_{i\sigma}$ . This Hamiltonian continues to be invariant under the  $SU(2)$  action induced by (19). Despite its similar appearance with the standard MF RVB result<sup>9</sup>, eq.(24) has a different content. First, it deals directly with the dopant-particle operators  $\Psi_{i\sigma}$ 's rather than with the electron operators  $c_{i\sigma}$ 's. In terms of  $\Psi_{i\sigma}$ 's,  $\hat{N}_e$  has a different representation, and a different equation for the chemical potential follows from that. Second, within our approach a nonzero  $\Delta$  directly implies superconductivity in contrast to the original BZA approach, where at half-filling  $\Delta^{BZA}$  is non-zero, but the state is insulating.

Due to the fact that we are directly dealing with the dopant particles  $T_c$  vanishes for  $\delta = 0$ . Moreover, the

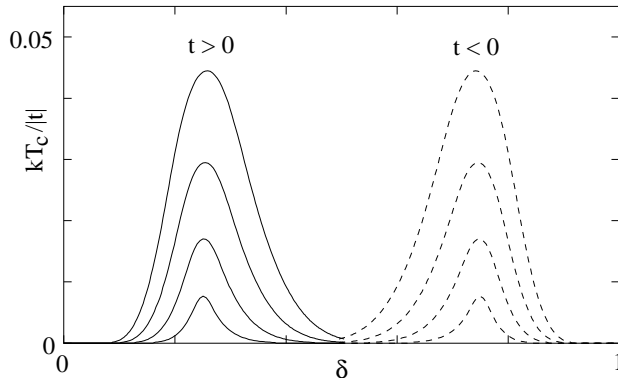


FIG. 1:  $T_c(\delta)$  for negative and positive  $t$ . The curves from the bottom to the top correspond to  $J/|t| = 0.6, 0.8, 1, 1.2$ .

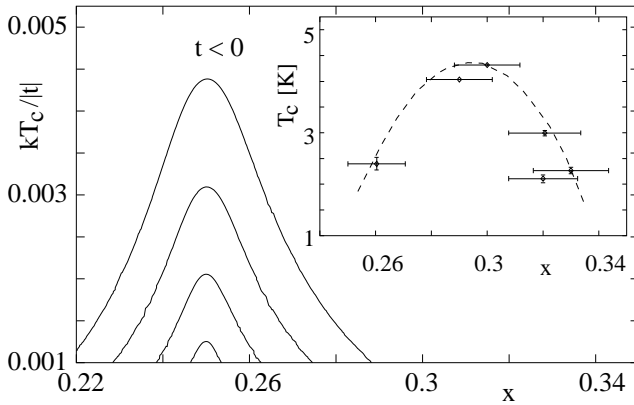


FIG. 2:  $T_c$  as a function of doping for  $t < 0$ . The curves from the bottom to the top correspond to  $J/|t| = 0.35, 0.4, 0.45, 0.5$ . For comparison, the insert shows experimental data for  $\text{Na}_x\text{CoO}_2 \cdot y\text{H}_2\text{O}$  taken from Ref.<sup>2</sup>.

average of the kinetic term in  $H_{t-J}^{SC} \sim t\delta$ . The increase of  $\delta$  reflects itself in the gain of kinetic energy which will eventually be of the order of  $J$ . When this occurs the singlet pairs tend to break up and the SC phase disappears. Strictly speaking  $T_c$  is non-zero for any non-vanishing  $\delta$  (see Fig. 1). This is an artifact of the MF approximation since it neglects a possible onset of magnetic ordering. In Figure 2 we use a cut-off at  $T = 1.0\text{K}$  and present the same temperature range seen in the inserted experimental data. As it was argued elsewhere<sup>7</sup> at sufficiently low temperature neither  $T_c$  nor  $\Delta$  can be observed experimentally.

A few remarks are in order. Since the RVB singlets are doped hole-hole pairs the present MF favors larger hole doping in contrast to the BZA scheme. Thus the present approach must be more reliable for the  $t-J$  interaction on a triangular lattice.

It can be shown (see Appendix) that the equations for the order parameter and the chemical potential that follow from the partition function representation (20) with the BCS hamiltonian (24) are invariant under the change

$t \rightarrow -t$ ,  $\delta \rightarrow 1 - \delta$ ,  $\mu \rightarrow -\mu$ . Thus the NDO constraint imposes within the MF BCS approximation a symmetry restriction on a possible structure of the phase diagram. Namely, the phase diagrams  $T_c(\delta)$  at  $t > 0$  and  $t < 0$  must be located symmetrically with respect to the point  $\delta = \frac{1}{2}$ . Any renormalization of the type  $t \rightarrow \delta t$ , frequently used in order to implement the NDO constraint, evidently spoils this symmetry and, therefore, can produce at most a phase diagram with an artificial agreement with experiment.

Finally, Eq. (24) corresponds to hole doping. However, as already mentioned earlier on, the  $\text{CoO}_2$ 's are more likely electron doped compounds. In order to deal with this case, within the representation (24), we make a canonical transformation  $\Psi_\sigma \rightarrow \Psi_{-\sigma}^+$  and keep the NDO constraint as before. In its new form the operator  $\Psi_\sigma^+$  creates a dopant electron. The phase diagram  $T_c \times \delta$  which follows from our new “dual” RVB scheme is shown in Fig.1, for hole doping. If we replace  $\delta \rightarrow x$ ,  $t \rightarrow -t$  we reproduce the main figure for the electron doping case. Our results for this case are shown in Fig.2. In the insert of this figure we reproduce the experimental data from Schaak et al<sup>2</sup> for comparison.

This phase diagram is evaluated directly from Eq. (24) considering a triangular lattice of  $\text{CoO}_2$ 's. The  $d + id$  symmetry of the MF OP predicted earlier in<sup>4,5</sup>, and<sup>18</sup> is employed throughout the calculations. Other symmetries can be tested if necessary using the same scheme. The representation (20) with the Hamiltonian function given by Eq. (24) incorporates the NDO constraint rigorously and tells us that at most one spinful fermion can live on a given lattice site. Technically, the problem reduces to a computation of the fermionic determinant in the presence of the constraints imposed by the  $\delta$ -functions.

The fermionic determinant arises upon integrating a bilinear form in the exponential over the complex spinors  $\Sigma_{\vec{k}, \varpi_n} \equiv \left( \bar{\Psi}_{\uparrow \vec{k}, \varpi_n}, \Psi_{\downarrow \vec{k}, -\varpi_n} \right)$ . Here  $\varpi_n = \frac{\pi}{\beta}(2n+1)$  stands for the Matsubara fermionic frequency and vector  $\vec{k} \in BZ$ . Had there been no  $\delta$ -function terms in (20) these amplitudes would have been completely independent. In the presence of the  $\delta$ -functions, however, only one set of those amplitudes (either that at  $\varpi_n > 0$  or at  $\varpi_n < 0$ ) can be picked out as the independent set of the integration variables. The second set of  $\Sigma$ 's then appears as a linear but highly nonlocal function of the first one. To simplify the problem we, at first, ignore the  $\delta$ -functions. Despite that, we take into account only one set of the modes,  $\Sigma_{\vec{k}, \varpi_n}$ ,  $\varpi_n > 0$ . This properly restricts the total number of the fermionic degrees of freedom. Note also that the same restricted set of the fermionic modes emerges in the MF treatment of the BCS hamiltonian for spinless fermions (see, e.g.,<sup>15</sup>).

Although this approximation cannot be justified rigorously, it goes beyond the one based on the renormalization of the hopping term in the form,  $t \rightarrow \delta t$ , which is frequently used to partly take into account the restriction

of no double occupancy. In particular, our approximation does not spoil the already mentioned symmetry of the phase diagram under the changes  $t \rightarrow -t$ ,  $\delta \rightarrow 1 - \delta$  dictated by the NDO constraint (see Fig. 1 and the Appendix). However, a more detailed analysis must take into account a rigorous treatment of the delta-function contribution.

Our results for  $\text{Na}_x\text{CoO}_2 \cdot y\text{H}_2\text{O}$  are very suggestive since for the first time the experimentally observed dome structure of the phase diagram is reproduced by theoretical calculations within a RVB framework. The obtained widths for the dome are also of the same magnitude as given by experiments<sup>2,3</sup>, although our doping values are somewhat shifted towards the origin. The precise value of  $J$  for this compound is still unknown. However for  $t = -0.1\text{eV}$  and  $J/|t|$  ranging from 0.35 to 0.5 as depicted in Figure 2,  $\max T_c$  varies roughly from  $1\text{K}$  to  $4\text{K}$ . Our mean field results are, therefore, in good agreement with the existing experimental data.

## VII. CONCLUSION

To conclude we developed a new RVB mean field theory which takes a direct account of the dopant carriers. These dopant particles are represented by appropriate fermion fields which carry both spin and charge and transform themselves as true  $\text{SU}(2)$  fundamental vectors. The resulting theory is written in a very convenient form since we are able in this way to consider the both doping dependence of the critical temperature as well as the kinetic energy effects which eventually destroy the superconductivity at larger dopings. By making a more extensive use of Hubbard operators we go beyond the conventional slave-boson approximation and take sufficient care of all symmetry properties of the hamiltonian model.

We initially applied this new RVB scheme to describe the superconducting properties observed in the cobaltates. We succeeded in getting qualitative good agreement with experiment. The dome structure of the phase diagram  $T_c \times \delta$  is well reproduced for the first time within a RVB framework. This is achieved without any symmetry violation of the t-J model for the whole doping regime.

While preparing this more extended version of our work we came across another RVB formulation in terms of dopant carriers<sup>19</sup>. Those authors use an extended t-J model with  $t$ ,  $t'$  and  $t''$  hopping parameters. In their scheme however those parameters are renormalized by interactions and this procedure automatically violates the underlying symmetries of the original t-J model.

As discussed in the Appendix, the MF phase diagram  $T_c(\delta)$  for the t-J model on the square lattice without frustration results in a max  $T_c$  located at  $\delta = 1/2$ . Although incorporating the next-nearest-neighbor (NNN) interaction in the kinetic term slightly shifts the diagram towards the origin, it cannot account for the experimen-

tally observed curve for the cuprates. It's clear that frustration is an important ingredient for the success of our RVB method. However, apart from that there is yet another important feature with needs to be taken into consideration to properly deal with the cuprates case. In the cuprates there are strong antiferromagnetic correlations which manifest themselves even inside the superconducting vortex cores. As a result the  $\langle \vec{S}_i \vec{M}_j \rangle$  correlations, which seem unimportant for the cobaltates, may also play an important role in the cuprates<sup>20</sup>. This will produce strong phase fluctuations which, most likely, need to be taken into account beyond mean field approximation. This work is in progress and will be presented elsewhere.

## Acknowledgments

One of us (E.K.) wants to acknowledge the hospitality of the ICCMP's staff and the financial support received from CAPES - Brazil.

## VIII. APPENDIX

In this Appendix we show that within the BCS MF approximation (24) the equations for the order parameter and the chemical potential are invariant under the change  $t \rightarrow -t$ ,  $\delta \rightarrow 1 - \delta$ ,  $\mu \rightarrow -\mu$ , provided the NDO constraint is rigorously taken into account.

First, we integrate out the fields  $\Psi_{\uparrow i}, \bar{\Psi}_{\uparrow i}$  in Eq. (20) with the hamiltonian function given by (24), which results in the effective action (15) with the classical Hamiltonian function now being,

$$H^{cl} = -t \sum_{ij} (\xi_i \bar{\xi}_j \langle z_i | z_j \rangle + h.c.) - \mu \left( N - \sum_i \bar{\xi}_i \xi_i \right) + \frac{J\Delta}{2} \sum_{ij} \left( \xi_i \xi_j \frac{\bar{z}_j - \bar{z}_i}{\sqrt{(1+|z_i|^2)(1+|z_j|^2)}} + h.c. \right). \quad (25)$$

Here  $z_i(t)$  and  $\xi_i(t)$  are dynamical fields. This representation rigorously incorporates the NDO constraint. Because of the rather complicated form of the action, we are in general unable to write out explicitly a quantum counterpart of hamiltonian (25) as a function of the  $\text{su}(2)$  spin generators and spinless  $\text{U}(1)$  fermionic operators. However, in the SC phase we get  $z_i(t) = z_i$ , which means that quantum fluctuations of the background spinon fields are totally ignored. In that case only the fermionic kinetic term is left in the action (15), and the quantum hamiltonian can be easily identified,

$$H = -t \sum_{ij} (f_i f_j^\dagger \langle z_i | z_j \rangle + h.c.) - \mu \left( N - \sum_i f_i^\dagger f_i \right) + \frac{J\Delta}{2} \sum_{ij} \left( f_i f_j \frac{\bar{z}_j - \bar{z}_i}{\sqrt{(1+|z_i|^2)(1+|z_j|^2)}} + h.c. \right). \quad (26)$$

The  $f_i$ 's stand for the on-site spinless fermionic operators, with  $\{f_i, f_j^\dagger\} = \delta_{ij}$  that correspond to the classical Grassmann amplitudes,  $f^{cl} = \xi$ , which give  $\{\xi_i, \bar{\xi}_j\} = 0$ . The dynamical spinon field  $z_i(t)$  loses its time-dependence and turns itself therefore into a sort of external classical  $c$ -valued spinon field.

Next, we evaluate the on-site free energy function,

$$F/N = -\frac{1}{N} \text{Tr} e^{-\beta H}, \quad (27)$$

where the symbol  $\text{Tr}$  is used to indicate the summation over the fermionic degrees of freedom as well as the complex  $c$ -valued spinon fields:

$$\text{Tr}(\cdots) := \int D\mu_{su(2)}(\bar{z}, z) \text{tr}_{f,f^\dagger}(\cdots) \quad (28)$$

The  $z$ -integral in (28) appears as an ordinary multiple integral. In this way the order parameter and chemical potential are determined by the conditions  $\partial F/\partial\Delta = 0$ ,  $\partial F/\partial\mu = \delta - 1$  which explicitly give

$$\left\langle \frac{J}{2} \sum_{ij} f_i f_j \frac{\bar{z}_j - \bar{z}_i}{\sqrt{(1+|z_i|^2)(1+|z_j|^2)}} + h.c. \right\rangle = 0, \quad (29)$$

and

$$\left\langle \frac{1}{N} \sum_i f_i^\dagger f_i \right\rangle = \delta, \quad (30)$$

respectively. Here  $\langle(\cdots)\rangle := \text{Tr}(\cdots)e^{-\beta H}/\text{Tr}e^{-\beta H}$ . It can be checked straightforwardly that eqs. (29) and (30) are invariant under the change  $t \rightarrow -t$ ,  $\mu \rightarrow -\mu$ ,  $\delta \rightarrow 1 - \delta$ . To see this one should simultaneously make the canonical transformation,  $f_i \rightarrow f_i^\dagger$ , and change the integration variables,  $z_i \rightarrow -\bar{z}_i$ . Accordingly, the phase diagrams  $T_c(\delta)$  at  $t > 0$  and  $t < 0$  are located symmetrically with respect to the point  $\delta = 1/2$ .

Explicitly, the equations for the order parameter and chemical potential read

$$\frac{1}{N} \sum_{\vec{k} \in BZ} \frac{\tanh(\frac{E_{\vec{k}}\beta}{2})}{E_{\vec{k}}} |\beta_{\vec{k}}|^2 = \frac{Z}{J}, \quad (31)$$

$$\frac{1}{2N} \sum_{\vec{k} \in BZ} \frac{\tanh(\frac{E_{\vec{k}}\beta}{2})}{E_{\vec{k}}} (t_{\vec{k}} - \mu) = \delta - 1/2, \quad (32)$$

where

$$E_{\vec{k}}^2 = (t_{\vec{k}} - \mu)^2 + J^2 \Delta^2 |\beta_{\vec{k}}|^2, \quad (33)$$

and  $t_{\vec{k}} = -2t\gamma_{\vec{k}}$ ,  $\gamma_{\vec{k}} = \sum_{\vec{n}} \cos \vec{k} \cdot \vec{n}$ . In the case of the 2D square lattice  $\gamma_{\vec{k}} = \cos k_x + \cos k_y$ , whereas  $\gamma_{\vec{k}} = \cos k_x + 2\cos(k_x/2)\cos(k_y\sqrt{3}/2)$  for the 2D triangular lattice. For the  $d_{x^2-y^2}$  pairing on the square lattice the phase factor

reads  $\beta_{\vec{k}} = \cos k_x - \cos k_y$ . For the triangular lattice we assume a  $d_1 + id_2$  symmetry of the order parameter<sup>4,5</sup>. Then,

$$\beta_{\vec{k}} = \cos k_x - \cos \frac{k_x}{2} \cos \frac{k_y\sqrt{3}}{2} + i\sqrt{3} \sin \frac{k_x}{2} \sin \frac{k_y\sqrt{3}}{2}. \quad (34)$$

The equations (31) and (32) are clearly seen to be invariant under the change  $t \rightarrow -t$ ,  $\mu \rightarrow -\mu$ ,  $\delta \rightarrow 1 - \delta$ , which results in the phase diagram depicted on Fig.1.

Note that the t-J hamiltonian on a square lattice with the nearest-neighbor (NN) interaction is invariant under the change,  $t \rightarrow -t$ . This is because this change amounts to a certain unitary transformation of the lattice electron operators. It then follows that the above two phase diagrams merge in this case into one, located at  $\delta = 1/2$ . Incorporating frustration (e.g., by taking into account the NNN interaction in the t-dependent term) destroys this symmetry and results in splitting of this diagram again into two located symmetrically with respect to the point  $\delta = 1/2$ . However for the generic values of the t-J parameters that splitting is rather small and cannot account for an experimentally observed phase diagram for the cuprates.

If we ignored completely the NDO constraint taking into account the modes  $\Sigma_{\vec{k}, \omega_n > 0}$  and  $\Sigma_{\vec{k}, \omega_n < 0}$  on equal grounds, we would get (on a square lattice) a diagram with  $\max T_c$  located at  $\delta = 1$ . This is markedly different from the NDO constraint-free BZA result, where  $\max T_c$  occurs at  $\delta = 0$ , which bears out that our theory is in a sense dual to the original BZA approach.

The conventional BZA MF theory formulated in terms of the lattice electron spin singlets with the renormalization  $t \rightarrow \delta t$  being implemented to partly incorporate the NDO constraint, however fails to maintain the symmetry of the phase diagram dictated by this constraint, and results in the same observation:  $\max T_c$  takes place again at  $\delta = 0$ , as in the constraint-free BZA theory. To see this consider the BZA MF hamiltonian<sup>9</sup>,

$$H_{t-J}^{BZA} = -t\delta \sum_{ij\sigma} c_{i\sigma}^\dagger c_{j\sigma} + h.c. - \mu \sum_{i\sigma} c_{i\sigma}^\dagger c_{i\sigma} + \frac{J\Delta}{2} \sum_{ij} (c_{i\uparrow} c_{j\downarrow} - c_{i\downarrow} c_{j\uparrow} + h.c.) + \frac{JNZ|\Delta|^2}{4}. \quad (35)$$

One obtains the following system of equations to determine the order parameter and chemical potential:

$$\frac{1}{N} \sum_{\vec{k}} \frac{\tanh(\frac{E_{\vec{k}}\beta}{2})}{E_{\vec{k}}} \gamma_{\vec{k}}^2 = \frac{Z}{2J}, \quad (36)$$

$$\frac{1}{N} \sum_{\vec{k}} \frac{\tanh(\frac{E_{\vec{k}}\beta}{2})}{E_{\vec{k}}} (t_{\vec{k}} - \mu) = \delta, \quad (37)$$

where

$$E_{\vec{k}}^2 = (t_{\vec{k}} - \mu)^2 + J^2 \Delta^2 \gamma_{\vec{k}}^2, \quad (38)$$

and  $t_{\vec{k}} = -2t\delta\gamma_{\vec{k}}$ ,  $\gamma_{\vec{k}} = \sum_{\vec{n}} \cos \vec{k}\vec{n}$ . The ensuing phase diagram  $T_c^{BZA}(\delta)$  is invariant under the change  $\delta \rightarrow -\delta$

so that  $\max T_c$  always occurs at  $\delta = 0$ .

---

<sup>1</sup> K. Takada, H. Sakurai, E. Takayama-Muromachi, F. Izumi, R. A. Dilanian, and T. Sasaki, *Nature* **422**, 53 (2003).

<sup>2</sup> R.E. Schaak, T. Klimczuk, M. L. Foo, and R. J. Cava, *Nature* **424**, 527 (2003).

<sup>3</sup> M. L. Foo, Y. Wang, S. Watauchi, H. W. Zandbergen, T. He, R. J. Cava, and N. P. Ong, *Phys. Rev. Lett.* **92**, 247001 (2004)

<sup>4</sup> G. Baskaran, *Phys. Rev. Lett.* **91**, 097003 (2003).

<sup>5</sup> B. Kumar and B. S. Shastry, *Phys. Rev. B* **68**, 104508 (2003).

<sup>6</sup> Q. -H. Wang, D. -H. Lee, and P. A. Lee, *Phys. Rev. B* **69**, 092504 (2004).

<sup>7</sup> O. I. Montrunich and P. A. Lee, *cond-mat/0310387*.

<sup>8</sup> G. Baskaran, *cond-mat/0306569*.

<sup>9</sup> G. Baskaran, Z. Zou, and P. W. Anderson, *Solid State Commun.* **63**, 973 (1987).

<sup>10</sup> M. U. Ubbens and P. A. Lee, *Phys. Rev. B* **49**, 6853 (1994).

<sup>11</sup> K. A. Chao, J. Spałek, and A. M. Oleś, *Phys. Rev. B* **18**, 3453 (1978).

<sup>12</sup> J. Hubbard, *Proc. R. Soc. London, Ser. A* **285**, 542 (1965).

<sup>13</sup> P. B. Wiegmann, *Phys. Rev. Lett.* **60**, 821 (1989).

<sup>14</sup> E.A. Kochetov and V.S. Yarunin, *Phys. Rev. B* **56**, 2703 (1997).

<sup>15</sup> E.A. Kochetov and M. Mierzejewski, *Phys. Rev. B* **61**, 1580 (2000).

<sup>16</sup> By a classical image of an operator algebra we mean its realization in terms of the Poisson brackets by functions on a classical phase space manifold.

<sup>17</sup> B. Lake, H.M. Rnnow, N.B. Christensen, K. Lefmann, G. Aeppli, D.F. McMorrow, N. Mangkorntong, M. Nohara, H. Takagi, T.E. Mason, P. Vorderwisch, P. Smeibidl, *Nature*, **415**, 299 (2002).

<sup>18</sup> C. Honerkamp, *Phys. Rev. B* **68**, 104510 (2003).

<sup>19</sup> Tiago C. Ribeiro and Xiao-Gang Wen, *arXiv:cond-mat/0410750*.

<sup>20</sup> Our approach properly accounts for the competition between superconductivity and the magnetic order. If the  $SU(2)$  symmetry is broken  $\langle \vec{S}_i \rangle \neq 0$ . Then, the MF hamiltonian (24) should be extended by the following term :  $\sum_i \vec{h}_i \vec{M}_i$ , where  $\vec{h}_i = -J \sum_{\langle j \rangle_i} \vec{S}_i$  and the summation is carried out over the neighboring sites. The magnetic order occurs in the hamiltonian in an analogous way as the magnetic field introduced by the Zeeman term. This interaction, when sufficiently strong, destroys superconductivity. Site dependence of the effective field  $\vec{h}_i$  depends on the lattice geometry. In the case of antiferromagnetic order on a square lattice  $\vec{h}_i$  represents a stagger magnetic field.